

## The osteoinductive effect of controlled bone morphogenic protein 2 release is location dependent

Olthof, Maurits G.L.; Lu, Lichun; Tryfonidou, Marianna A.; Loozen, Loek D.; Pourn, Behdad; Yaszemski, Michael J.; Meij, Björn P.; Dhert, Wouter J.A.; Alblas, Jacqueline; Kempen, Diederik H.R.

**DOI**

[10.1089/ten.tea.2017.0427](https://doi.org/10.1089/ten.tea.2017.0427)

**Publication date**

2019

**Document Version**

Final published version

**Published in**

Tissue Engineering - Part A

**Citation (APA)**

Olthof, M. G. L., Lu, L., Tryfonidou, M. A., Loozen, L. D., Pourn, B., Yaszemski, M. J., Meij, B. P., Dhert, W. J. A., Alblas, J., & Kempen, D. H. R. (2019). The osteoinductive effect of controlled bone morphogenic protein 2 release is location dependent. *Tissue Engineering - Part A*, 25(3-4), 193-202. <https://doi.org/10.1089/ten.tea.2017.0427>

**Important note**

To cite this publication, please use the final published version (if applicable). Please check the document version above.

**Copyright**

Other than for strictly personal use, it is not permitted to download, forward or distribute the text or part of it, without the consent of the author(s) and/or copyright holder(s), unless the work is under an open content license such as Creative Commons.

**Takedown policy**

Please contact us and provide details if you believe this document breaches copyrights. We will remove access to the work immediately and investigate your claim.

**ORIGINAL ARTICLE**

---

# The Osteoinductive Effect of Controlled Bone Morphogenic Protein 2 Release Is Location Dependent

Maurits G.L. Olthof, MD,<sup>1-5</sup> Lichun Lu, PhD,<sup>2,3</sup> Marianna A. Tryfonidou, DVM, PhD,<sup>4</sup> Loek D. Loozen, MD, PhD,<sup>1</sup> Behdad Pouran, PhD,<sup>1,6</sup> Michael J. Yaszemski, MD, PhD,<sup>2,3</sup> Björn P. Meij, DVM, PhD,<sup>4</sup> Wouter J.A. Dhert, MD, PhD,<sup>1,4</sup> Jacqueline Alblas, PhD,<sup>1</sup> and Diederik H.R. Kempen, MD, PhD<sup>7</sup>

The main challenge in bone morphogenic protein 2 (BMP-2)-based application lies in finding strategies that prolong its effective period as it has a short biological half-life. Several BMP-2 release profiles have shown to enhance bone formation at various application sites. However, it remains to be determined which BMP-2 release profile best augments bone formation and whether this effect is location dependent. Therefore, the aim of this study was to investigate the effect of BMP-2 release from oligo[(polyethylene glycol) fumarate] bis(2-(methacryloyloxy)ethyl) phosphate (OPF-BP) composites on the osteoinductive efficacy at ectopic versus orthotopic application. By varying the BMP-2 loading method, three different OPF-BP composites were created with varied release profiles. The composites were compared with unloaded OPF-BP as negative control, and to the clinically used Infuse<sup>®</sup> absorbable collagen sponge (ACS) as positive control. Bone formation was assessed by microcomputed tomography after 9 weeks of subcutaneous implantation and 3, 6, and 9 weeks of orthotopic implantation in rats ( $n=48$ ). Whereas a BMP-2 burst release of >49% generated significantly more bone compared with sustained release (burst release <30%) at the subcutaneous implantation site, differential release did not affect bone formation at the orthotopic site. Furthermore, all BMP-2 containing OPF-BP composites showed significantly more bone formation compared with ACS in the orthotopic implantation site. In conclusion, this study clearly shows that the osteoinductive effect of different BMP-2 release profiles is location dependent. In addition, more bone formation in OPF-BP compared with ACS at both application sites emphasizes the role of biomaterials as a scaffold to achieve proper bone tissue formation.

**Keywords:** bone tissue engineering, bone morphogenetic protein 2, oligo[(polyethylene glycol) fumarate], application sites

## Impact Statement

The main challenge in bone morphogenic protein 2 (BMP-2)-based application lies in finding strategies to prolong its biologic activity as it has a short biological half-life. The present study uses a phosphate-modified oligo[(polyethylene glycol) fumarate] hydrogel that can be tuned to achieve differential release profiles of biologically active BMP-2 release. We demonstrate that this platform outperforms Infuse<sup>®</sup>, currently used in the clinic and that the osteoinductive effect of BMP-2 is location dependent. Altogether, this study stresses the importance of evaluating efficacy of bone tissue engineering strategies at an orthotopic location rather than subcutaneously. Even more so, it emphasizes the role of biomaterials as a scaffold to achieve proper bone tissue engineering.

---

<sup>1</sup>Department of Orthopaedics, University Medical Center, Utrecht, The Netherlands.

Departments of <sup>2</sup>Physiology and Biomedical Engineering and <sup>3</sup>Orthopedic Surgery, Mayo Clinic College of Medicine, Rochester, Michigan.

<sup>4</sup>Department of Clinical Sciences of Companion Animals, Faculty of Veterinary Medicine, Utrecht University, Utrecht, The Netherlands.

<sup>5</sup>Department of Orthopaedics, Balgrist University Hospital, University of Zurich, Zurich, Switzerland.

<sup>6</sup>Department of Biomechanical Engineering, Faculty of Mechanical, Maritime, and Materials Engineering, Delft University of Technology (TU Delft), Delft, The Netherlands.

<sup>7</sup>Department of Orthopaedic Surgery, Onze Lieve Vrouwe Gasthuis, Amsterdam, The Netherlands.

## Introduction

**B**ONE MORPHOGENIC PROTEIN 2 (BMP-2), a well-known osteoinductive growth factor, has shown great potential in numerous animal models.<sup>1</sup> The main challenge in BMP-2-based application lies in finding strategies that prolong its biological effective period as it has a short biological half-life.<sup>2</sup> Therefore, biomaterials are used as delivery vehicles to improve the local retention and osteoinductive capacity of BMP-2 compared with locally injected carrier-free BMP-2.<sup>3–6</sup> Several biomaterials with differential growth factor release kinetics have shown to enhance BMP-2-induced bone formation at various application sites, including ectopic sites (subcutaneous, intramuscular) and orthotopic sites such as segmental defects (femur, fibula, humerus, radius, tibia), drill defects (calvaria, cleft, condyle, patella, vertebrae), and lumbar fusion models.<sup>7</sup> However, it remains to be determined which BMP-2 release profile best augments bone formation and whether this effect is location dependent.

Determining the biologic effect of the released BMP-2 is complicated by confounding factors influencing bone formation, including the biomaterial characteristics of the delivery vehicle.<sup>8</sup> While many previous studies investigated the effect of *in vitro* BMP-2 release on bone formation, the value of these results is limited since *in vitro* BMP-2 release cannot be extrapolated to *in vivo* release.<sup>4,8–14</sup> Other studies that investigated the effect of *in vivo* BMP-2 release on bone formation did not address the confounding effect of biomaterial characteristics on bone formation.<sup>9,15,16</sup> In studies where the need for BMP-2 release from biomaterials with similar characteristics was recognized, either no differential release pattern could be obtained<sup>17</sup> or the biological activity of the released BMP-2 was not investigated.<sup>12</sup>

Therefore, in a previous study, we developed a composite consisting of oligo[(polyethylene glycol) fumarate] bis(2-(methacryloyloxy)ethyl) phosphate hydrogel (OPF-BP) containing poly(lactic-co-glycolic acid) (PLGA) microspheres capable of releasing biologically active BMP-2 with several *in vivo* release profiles while maintaining similar scaffold chemistry and structure.<sup>18</sup> *In vitro* analysis of the phosphorylated OPF-BP hydrogel showed improved cellular attachment and mineralization compared with unmodified polyethylene glycol (PEG)-based hydrogels.<sup>19–22</sup> Furthermore, the phosphate-modified surface improved BMP-2-induced bone formation and osteoconductivity *in vivo*.<sup>23</sup> The BMP-2 release from this composite can be altered by varying the BMP-2 adsorption/microsphere encapsulation ratio. Whereas a BMP-2 burst release of >49% in OPF-BP hydrogels showed appropriate bone formation, a more sustained release of BMP-2 (burst release <25%) generated only minimal calcifications in a subcutaneous rat model.<sup>18</sup> Although this sub-

cutaneous model provides valuable information about BMP-2 retention profiles and ectopic osteoinductivity, it remains unknown whether this ectopic osteoinductive capacity also applies in orthotopic locations. Furthermore, differences in cellular availability and matrix and growth factor composition at an orthotopic application site could influence the efficacy of the various BMP-2 release profiles.<sup>24</sup> Therefore, the aim of this study is to investigate the effect of BMP-2 release from OPF-BP composites on the osteoinductive efficacy at ectopic versus orthotopic application.

## Materials and Methods

### Experimental design

To investigate the location-dependent effect of differential BMP-2 release on bone formation, composites loaded with a total of 2  $\mu$ g recombinant human BMP-2 (Medtronic, Minneapolis, MN) with tailorable BMP-2 release were implanted ectopically (subcutaneously) and orthotopically (critical-sized femoral defect) in rats. All composites consisted of an OPF-BP hydrogel (22.5% w/w) containing PLGA microspheres (2.5% w/w) with 75% w/w NaCl particles to create porosity. By varying the BMP-2 loading method, three different implants were created consisting of 100% of the BMP-2 encapsulated in PLGA microspheres (OPF-BP-MS: Microspheres,  $\pm$ 30% burst release), 50% of the BMP-2 encapsulated in PLGA microspheres, 50% adsorbed on the composite (OPF-BP-Cmb: Combined,  $\pm$ 49% burst release), and 100% adsorbed on the composite (OPF-BP-Ads: Adsorbed,  $\pm$ 85% burst release)<sup>18</sup> (Table 1 and Supplementary Fig. S1).

The composites were compared with unloaded OPF-BP (OPF-BP) as negative control, and with the clinically used Infuse<sup>®</sup> absorbable collagen sponge (ACS) containing 2  $\mu$ g adsorbed recombinant human BMP-2 for both orthotopic and ectopic locations as positive control. For the orthotopic site, an additional group was added (defect only, without implant augmentation) to confirm that the femoral defect was critical sized. Bone formation was assessed using microcomputed tomography (micro-CT) after 9 weeks of subcutaneous implantation and after 3, 6, and 9 weeks of orthotopic implantation.

### Microsphere fabrication

PLGA (50:50 lactic to glycolic acid ratio,  $M_w$  52 kDa; Evonik, AL) microspheres were fabricated using a water-in-oil-in-water (W1–O–W2) double emulsion solvent extraction technique according to a previously described method.<sup>25</sup> Briefly, 100  $\mu$ L of 4 mg/mL BMP-2 solution, 50  $\mu$ L of 4 mg/mL BMP-2 solution, or 100  $\mu$ L of distilled deionized water (ddH<sub>2</sub>O) was emulsified with 250 mg PLGA 50:50

TABLE 1. COMPOSITE CHARACTERISTICS

	Porosity (w/w)	PLGA Msp (w/w)	BMP-2 loading	BMP-2 release
OPF-BP-MS	75%	2.5%	100% MS	$\pm$ 30% burst release
OPF-BP-Cmb	75%	2.5%	50% MS, 50% Ads	$\pm$ 49% burst release
OPF-BP-Ads	75%	2.5%	100% Ads	$\pm$ 85% burst release

OPF-BP, oligo[(polyethylene glycol) fumarate] bis(2-[methacryloyloxy]ethyl) phosphate; PLGA, poly(lactic-co-glycolic acid); BMP-2, bone morphogenetic protein-2; MS, microsphere (more sustained BMP-2 release); Cmb, combined (combined BMP-2 release); Ads, adsorbed (mainly burst release).

dissolved in 1.25 mL of dichloromethane using a vortex at 3050 rpm to create PLGA microspheres loaded with 1.36  $\mu\text{g}$  BMP-2/mg PLGA (OPF-BP-MS), 0.68  $\mu\text{g}$  BMP-2/mg PLGA (OPF-BP-Cmb), and unloaded microspheres (OPF-BP-Ads), respectively. The solution was re-emulsified in 2 mL of 2% (w/v) aqueous poly(vinyl alcohol) (PVA, 87–89% mole hydrolyzed, Mw = 13,000–23,000; Sigma Aldrich) to create the double emulsion and added to 100 mL of a 0.3% (w/v) PVA solution and 100 mL of a 2% (w/v) aqueous isopropanol solution. After 1 h of slowly stirring, the resulting PLGA microspheres were collected by centrifugation at 2500 rpm for 3 min, washed three times with ddH<sub>2</sub>O, and freeze-dried to a free-flowing powder. The characteristics of the PGLA microspheres have been reported in a previous study.<sup>18</sup>

#### Fabrication of composites

OPF was synthesized using PEG with an initial molecular weight of 10 kDa according to a previously described method.<sup>20</sup> BP (Aldrich, Milwaukee, WI) was crosslinked into the OPF hydrogel. The OPF-BP hydrogel and the composites were fabricated according to a previously described method.<sup>18</sup> To create the OPF-BP hydrogel, OPF (41% w/w), *N*-vinyl pyrrolidone (NVP, 29% w/w; Sigma Aldrich, St. Louis, MO), BP (8.2% w/w), and Irgacure 2959 (0.2% w/w; Ciba-Specialty Chemicals, Tarrytown, NY) were dissolved in deionized water (21.6% w/w). To create the composites, the OPF/NVP/BP paste (22.5% w/w) was mixed with NaCl salt particles (75% w/w, sieved to a maximum size of 300  $\mu\text{m}$ ) and PLGA microspheres (2.5% w/w). The resulting mixture was forced into a cylindrical mold with dimensions of 3.0 mm diameter and 5.0 mm length and exposed to a UV light (UV-Handleuchte lamp A, Hartenstein, Germany, wavelength: 365 nm, intensity: 1.2 mW/cm<sup>2</sup>, distance: 3 cm) to crosslink for 40 min. The composites were collected (59.7  $\pm$  0.5 mg dry weight, 0.03  $\mu\text{g}$  BMP-2/composite) and immersed in sterile water to leach out the salt. After blot drying, additional BMP-2 was loaded on the composite matrix by adsorption for the OPF-BP-Cmb and the OPF-BP-Ads scaffolds.

By varying the BMP-2 loading method, three different implants were created consisting of 100% of the BMP-2 encapsulated in PLGA microspheres (OPF-BP-MS,  $\pm$ 30% burst release), 50% of the BMP-2 encapsulated in PLGA microspheres and 50% adsorbed on the composite (OPF-BP-Cmb,  $\pm$ 49% burst release), and 100% adsorbed on the composite (OPF-BP-Ads,  $\pm$ 85% burst release).<sup>18</sup> The loss of BMP-2 by the fabrication method was objectivized in a previous study.<sup>18</sup> This calculation was used to estimate the BMP-2 loss and adjust the applied amount by adsorption. A similar BMP-2 dose and composite fabrication method were used for all OPF-BP composites, which resulted in  $\sim$ 2  $\mu\text{g}$  BMP-2/implant.<sup>18</sup> The release profiles of the three different BMP-2 loading methods are shown in Supplementary Figure S1. Although this different incorporation process could influence BMP-2 bioactivity, the released BMP-2 remained to show *in vitro* bioactivity compared with a freshly added BMP-2 dose to the cell cultures.<sup>18</sup> The Infuse ACS was cut into cylindrical (4 mm in diameter and 6 mm in length) rods using a tissue puncher and adsorbed with 2  $\mu\text{g}$  BMP-2/implant. The characteristics of OPF-BP have been investigated in detail in a previous study.<sup>18,20</sup>

#### Animals and surgical procedure

Forty-eight 16.0  $\pm$  1.2-week-old male Sprague Dawley rats (Envigo, Horst, NL) were used in this study according to an approved protocol by the Dutch Central Committee for Animal Care and Use (protocol: AVD115002015111). Before surgery, antibiotic prophylaxis (Terramycin/LA, 60 mg/kg; Pfizer, NL) and analgesia (Temgesic, 0.05 mg/kg) were given subcutaneously. Surgery was performed under sterile conditions and general inhalation anesthesia (isoflurane: induction 4%, maintenance  $\sim$ 1.5%). For the orthotopic site, the femur was exposed by a lateral approach, and a polyether ether ketone plate (length: 2.3 cm, thickness: 3 mm, width: 3 mm and six holes) was fixed to the cranial site of the femur using three screws (length: 7 mm, diameter 1 mm) at the proximal end and three screws (length: 7 mm, diameter 1 mm) at the distal end of the plate. The periosteum over  $\sim$ 8 mm of the screw-free mid-diaphysis was removed before removal of a 6-mm-long bone segment using a tailor-made saw guide and a wire saw (RatFix; AO Foundation).

Following closure of the femoral wound, the ectopic site was prepared. Subcutaneous pockets were created in the thoracolumbar region and filled with implants corresponding to the orthotopic defect. In the group of rats with the empty orthotopic defect, an unloaded OPF-BP scaffold was implanted subcutaneously. Temgesic (0.05 mg/kg) was given subcutaneously as postoperative analgesia two times daily for 3 days.

#### Quantification of bone volume

micro-CT was used to determine the total bone volume within the scaffolds in the orthotopic and ectopic location. *In vivo* scanning under general anesthesia (isoflurane 1.5–4%) was performed at 3, 6, and 9 weeks using a quantum FX (PerkinElmer) scanner at 42  $\mu\text{m}^3$  voxel size, 3-min scan time, 90 kV voltage, and 180  $\mu\text{A}$  current. *Ex vivo* scanning after 9 weeks was performed to analyze the subcutaneous implants. Global thresholding was applied in ImageJ (version 2.0.0-rc-43/1.51f) to quantify bone formation (BoneJ, plugin of ImageJ) within the implants. The osteoinductive efficacy of the released BMP-2 was analyzed by normalizing the bone volume over the assumed% BMP-2 release based on the previously studied subcutaneous rat model after 3, 6, and 9 weeks.<sup>18</sup> The change in bone volume over time is calculated in bone volume increase/week for every 3 weeks.

#### Histology

After micro-CT, tissues were fixed in formalin and samples were dehydrated in graded series of ethanol and embedded in methyl methacrylate. Qualitative assessment was performed in 30  $\mu\text{m}$  methylene blue/basic fuchsin-stained sections for evaluation of general tissue response and bone formation.

#### Statistical analysis

Statistical analysis was performed using SPSS 22.0 (SPSS, Inc., Chicago, IL). Before the *in vivo* study, power analysis estimated that a sample size of  $n = 8$  was needed to demonstrate a relevant difference of at least 20% at an alpha of 0.05, standard deviation (SD) of 1.4, and a power of 80%. *In vivo* results ( $n = 8$ ) are represented as means  $\pm$  SDs. All

data sets were tested for outliers using Hoaglin's outlier labeling rule,<sup>26</sup> for normality of the residuals using the Shapiro-Wilk test, and for homogeneity of variances using the Levene's test. Parametric data were analyzed with univariate analysis of variances and Benjamini-Hochberg *post-hoc*. Differences were considered significant for  $p < 0.05$ .

## Results

### Animals

In one rat in the unloaded OPF-BP group, implant failure occurred during postmortem preparation for the micro-CT. Therefore, this sample was excluded from the 9-week analysis. The other rats showed no complications and remained healthy during the 9-week follow-up.

### Analysis of the bone volume

In the orthotopic application, an increasing amount of bone was seen in all defects macroscopically (Fig. 1). The bone was formed as a compact shell at the cortical region and had a trabecular structure in the center. None of the empty defects and defects filled with an unloaded implant showed bridging of the defect on the micro-CT images. Furthermore, whereas OPF-Cmb and OPF-BP-Ads showed bridging of the defects mainly consisting out of a compact shell, OPF-BP-MS showed more trabecular structures bridging the defect. For ACS, no bridging of the defects was observed.

Quantification of the bone volume using micro-CT showed a significantly ( $p < 0.01$ ) higher bone volume in all BMP-2 containing implants compared with the negative

controls (empty defect and unloaded OPF-BP) after 3 weeks (Fig. 2). For the negative controls, the bone volume in the empty defect ( $13.5 \pm 5.6 \text{ mm}^3$ ) was significantly ( $p < 0.01$ ) higher compared with the defects containing unloaded OPF-BP ( $8.0 \pm 2.7 \text{ mm}^3$ ) after 3 weeks. In the BMP-2-loaded implants, significantly ( $p < 0.03$ ) more bone was observed in OPF-BP-Cmb ( $63.3 \pm 24.6 \text{ mm}^3$ ) compared with OPF-BP-MS ( $41.2 \pm 14.6 \text{ mm}^3$ ) in the first 3 weeks.

After 6 weeks, all BMP-2-loaded implants showed a higher ( $p < 1E^{-7}$ ) bone volume (OPF-MS:  $99.1 \pm 22.0 \text{ mm}^3$ , OPF-Cmb:  $122.2 \pm 14.2 \text{ mm}^3$ , OPF-Ads:  $130.6 \pm 23.4 \text{ mm}^3$ , and ACS:  $65.8 \pm 21.6 \text{ mm}^3$ ) compared with the negative controls (empty defect:  $19.9 \pm 8.1 \text{ mm}^3$  and unloaded OPF-BP:  $17.9 \pm 6.6 \text{ mm}^3$ ) (Fig. 2). All femoral defects containing BMP-2-loaded OPF-BP composites showed a higher ( $p < 0.001$ ) bone volume compared with ACS. Furthermore, differences were observed within the BMP-2-loaded OPF-BP composites with OPF-BP-Ads and OPF-BP-Cmb generating a higher ( $p < 0.04$ ) bone volume compared with OPF-BP-MS.

At 9-week follow-up, the defects containing BMP-2-loaded OPF-BP composites contained a higher ( $p < 1.4E^{-6}$ ) bone volume compared with the empty defects, unloaded OPF-BP controls, and ACS. There were no differences between BMP-2 containing OPF-BP composites (OPF-MS:  $122 \pm 19.0 \text{ mm}^3$ , OPF-Cmb:  $129.5 \pm 8.6 \text{ mm}^3$ , and OPF-Ads:  $140.1 \pm 11.7 \text{ mm}^3$ ). ACS contained more ( $p < 1E^{-6}$ ) bone volume ( $71.9 \pm 24.0 \text{ mm}^3$ ) compared with the negative controls (empty defect:  $24.0 \pm 9.1 \text{ mm}^3$  and unloaded OPF-BP:  $25.9 \pm 9.8 \text{ mm}^3$ ). Three-dimensional (3D) micro-CT reconstructions of the bone defects after 3, 6, and 9 weeks showed a similar pattern as the bone volume measurements (Fig. 1).

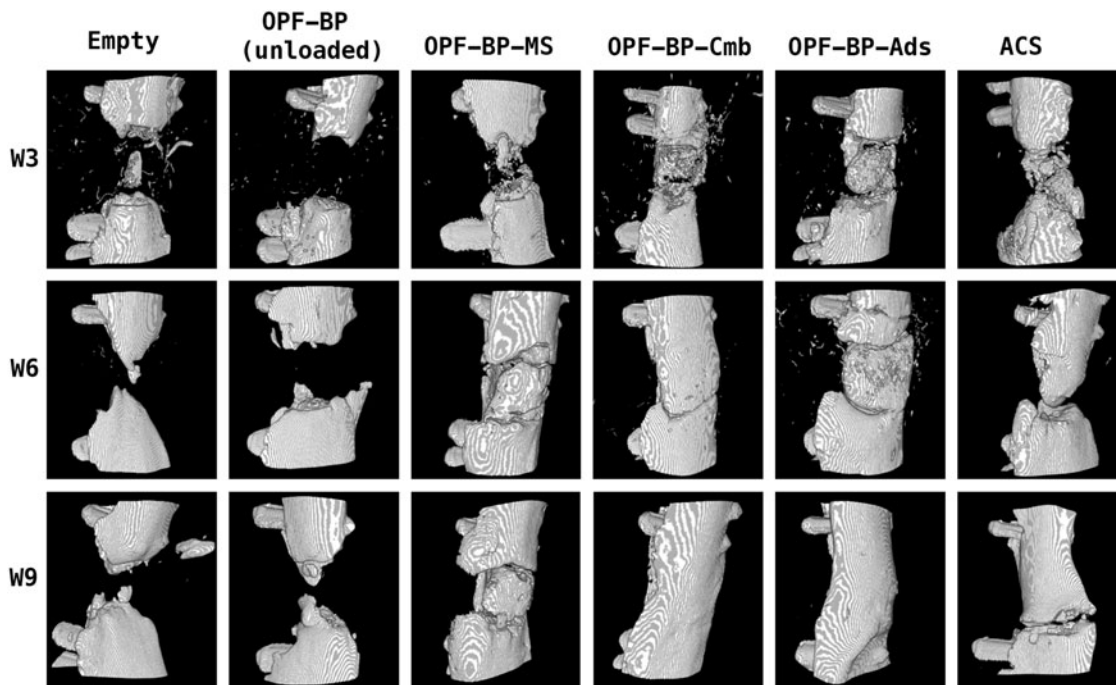


**FIG. 1.** Three-dimensional micro-CT reconstructions of the bone defects after 3, 6, and 9 weeks. Empty: unfilled defect, OPF-BP: unloaded control, OPF-BP-MS: microsphere (more sustained BMP-2 release), OPF-BP-Cmb: combined (combined BMP-2 release), OPF-BP-Ads: adsorbed (mainly burst release), ACS: absorbable collagen sponge containing  $2 \mu\text{g}$  BMP-2 (mainly burst release) as positive control. micro-CT, microcomputed tomography; OPF-BP, oligo[(polyethylene glycol) fumarate] bis(2-(methacryloyloxy)ethyl) phosphate; BMP-2, bone morphogenic protein.

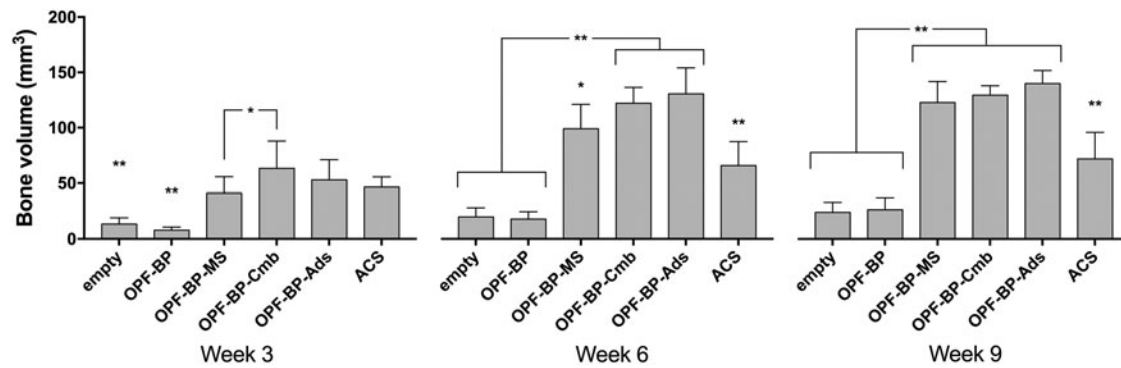


**FIG. 2.** Newly formed bone in the orthotopic defect after 3, 6, and 9 weeks shown in volume mean  $\pm$  SD (mm<sup>3</sup>). \* $p < 0.05$  and \*\* $p < 0.01$ : significantly different from all other groups or between specified groups when accompanied by an *asterisk bracket*. Empty: unfilled defect, OPF-BP: unloaded control, OPF-BP-MS: microsphere (more sustained BMP-2 release), OPF-BP-Cmb: combined (combined BMP-2 release), OPF-BP-Ads: adsorbed (mainly burst release), ACS: absorbable collagen sponge containing 2  $\mu$ g BMP-2 (mainly burst release) as positive control. SD, standard deviation.

To analyze osteoinductive efficacy of the released BMP-2 from OPF-BP composites and ACS, the bone volume was normalized based on the % released BMP-2 after 3, 6, and 9 weeks of implantation (Fig. 3A). After 3 weeks, OPF-BP-Cmb and OPF-BP-MS showed significantly ( $p < 0.01$ )

higher bone volume per released BMP-2 compared with OPF-BP-Ads and ACS. Subsequently, after 6 and 9 weeks of implantation, all BMP-2 containing OPF-BP composites showed significantly ( $p < 4E^{-6}$ ) more bone as a function of the released BMP-2 compared with ACS.

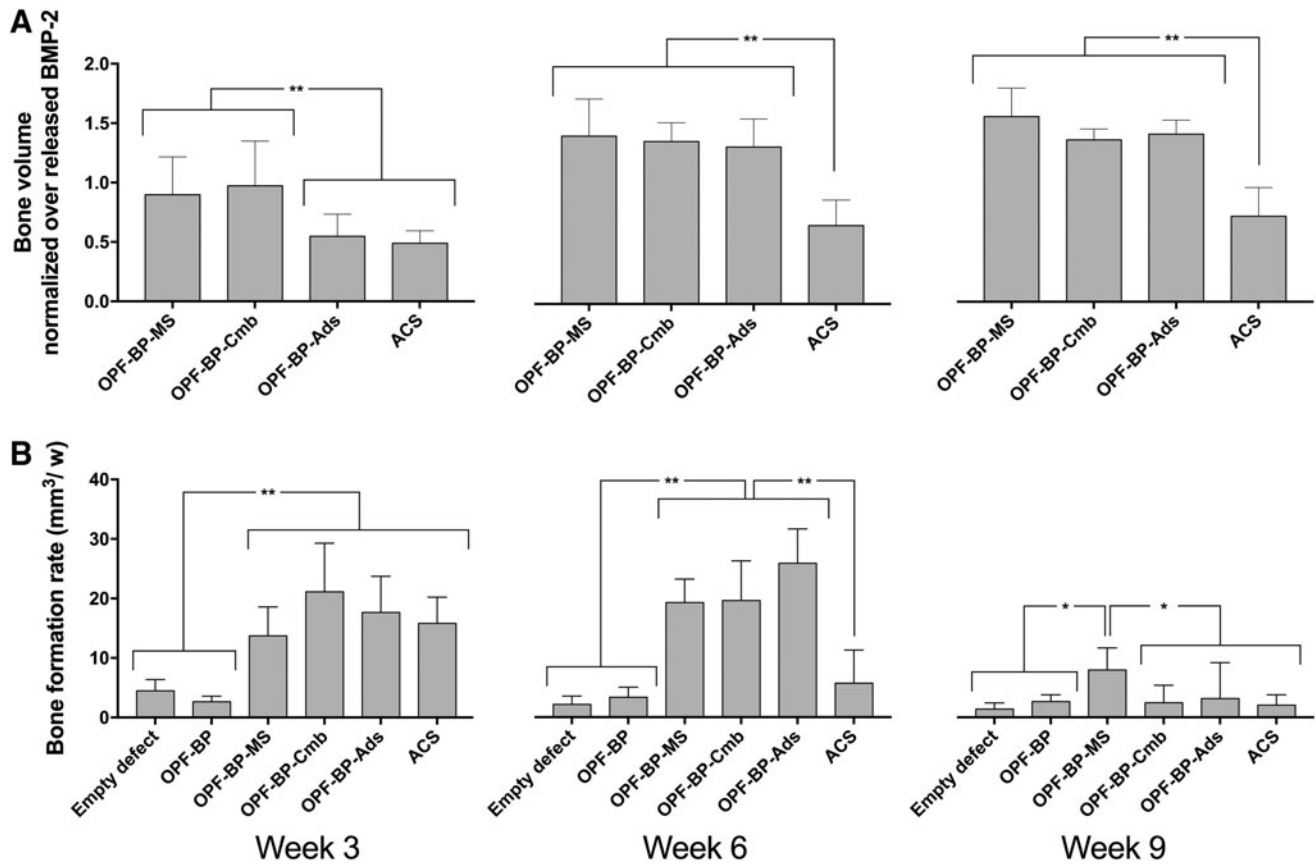


**FIG. 3.** Newly formed bone in the orthotopic defect normalized over % released BMP-2 after 3, 6, and 9 weeks shown in volume/% BMP-2 mean  $\pm$  SD (mm<sup>3</sup>%) (A). Bone formation rate in the orthotopic defect every 3 weeks (mm<sup>3</sup>/week) (B). \* $p < 0.05$  and \*\* $p < 0.01$ : significantly different from all other groups or between specified groups when accompanied by an *asterisk bracket*. Empty: unfilled defect, OPF-BP: unloaded control, OPF-BP-MS: microsphere (more sustained BMP-2 release), OPF-BP-Cmb: combined (combined BMP-2 release), OPF-BP-Ads: adsorbed (mainly burst release), ACS: absorbable collagen sponge containing 2  $\mu$ g BMP-2 (mainly burst release) as positive control.

To estimate bone formation rates, the difference in bone volume within each group between time points was calculated (Fig. 3B). After 3 weeks, all BMP-2 containing implants showed a higher ( $p < 0.01$ ) bone formation rate compared with the controls. For the 6-week time point, the bone formation rate of the BMP-2 containing OPF-BP implants was higher ( $p < 0.008$ ) compared with ACS and negative controls. After 9 weeks of implantation, OPF-BP-MS showed a faster ( $p < 0.03$ ) bone formation compared with all other implants.

After 9 weeks of subcutaneous implantation, a different pattern was seen compared with orthotopic implantation on 3D micro-CT reconstructions (Fig. 4A) and bone volume measurements (Fig. 4B). For the BMP-2-loaded implants, OPF-BP-Cmb ( $28.2 \pm 17.0 \text{ mm}^3$ ) and OPF-BP-Ads ( $35.6 \pm 22.8 \text{ mm}^3$ ) contained a higher ( $p < 0.005$ ) bone volume compared with OPF-BP-MS ( $6.3 \pm 5.4 \text{ mm}^3$ ) and ACS ( $6.0 \pm 3.2 \text{ mm}^3$ ). The unloaded OPF-BP composites contained no bone (not depicted in Fig. 4).

### Histology

After 9 weeks of orthotopic implantation, there was interposition of muscle tissue in the center of the empty femoral defect with limited ingrowth of woven bone from the distal and proximal osteotomy sides (Fig. 5). The unloaded OPF-BP composites were surrounded by a fibrous

capsule and showed ingrowth of fibrous tissue ( $>75\%$  pore volume) in the pores of the scaffold with bone formation at both osteotomy sides. In all BMP-2-loaded OPF-BP composites, a combination of endochondral, woven, and lamellar bone formation ( $>75\%$  pore volume) was observed with fat cells centrally in the pores. The exterior of the BMP-2 containing OPF-BP composites was surrounded by a bony cortex. Bone formation was located on the surface of the OPF-BP composite and in the center of the pores of the scaffold. The ACS was fully resorbed and the defect was mainly filled with woven and lamellar bone ( $>50\%$ ).

After 9 weeks of subcutaneous implantation, the unloaded OPF-BP composites were surrounded by a fibrous capsule with fibrous tissue ingrowth ( $>50\%$  pore volume) and no bone formation (Fig. 6). In both OPF-BP-Ads and OPF-BP-Cmb composites, woven bone and fat tissue were observed in the pores ( $>50\%$  pore volume) with a bony and fibrous layer surrounding the implants. Woven and lamellar bone was seen lying on the surface of pores and centrally in the pores. A combination of woven bone, fat tissue, and fibrous tissue was observed in the pores ( $>50\%$  pores volume) of the OPF-BP-MS composites with a bony and fibrous layer surrounding the implant. The ACS was fully resorbed and showed small ossicles consisting of lamellar and woven bone and fat tissue. The bone in the center of these ossicles had a trabecular structure with fat tissue filling the void spaces in the trabeculae.

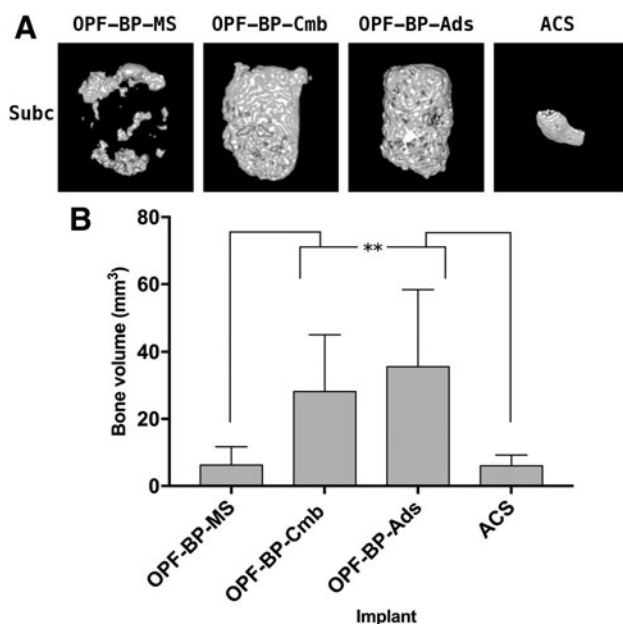


**FIG. 4.** Three-dimensional micro-CT reconstructions of the BMP-2 containing implants after 9 weeks of subcutaneous implantation (A). Newly formed bone after 9 weeks of subcutaneous implantation shown in volume mean  $\pm$  SD ( $\text{mm}^3$ ) (B). \*\* $p < 0.01$ : significantly different from all other groups or between specified groups when accompanied by an asterisk bracket. OPF-BP: unloaded control, OPF-BP-MS: microsphere (more sustained BMP-2 release), OPF-BP-Cmb: combined (combined BMP-2 release), OPF-BP-Ads: adsorbed (mainly burst release), ACS: absorbable collagen sponge containing  $2 \mu\text{g}$  BMP-2 (mainly burst release) as positive control.

### Discussion

This study clearly showed that the osteoinductive effect of BMP-2 release profiles was location dependent. Whereas BMP-2 burst release generated significantly more bone compared with sustained release at a subcutaneous implantation site, bone formation was not different between scaffolds effectuating different BMP-2 release profiles in orthotopic implantation. Furthermore, all BMP-2 containing OPF-BP composites showed significantly more bone formation compared with ACS at the orthotopic implantation site, while subcutaneously this effect was only seen for composites with a BMP-2 burst release of  $>49\%$ .

The application sites influenced the effect of BMP-2 release profiles on bone formation. To compare the effect of BMP-2 release profiles on bone formation in an orthotopic compared with an ectopic location, OPF-BP scaffolds with tailorable BMP-2 release profiles were used.<sup>18</sup> Whereas adsorption of the growth factor on the composites resulted in a large burst release of more than 85% within the first 3 days, loading of BMP-2 in microspheres generated a lower burst release of  $<30\%$  with a more sustained release for the rest of the 9-week period.<sup>18</sup> In the ectopic location, a burst release of BMP-2 was associated with efficient bone formation: OPF-BP composites effectuating primarily burst release generated significantly more bone compared with OPF-BP composites with a sustained release. However, no significant differences in bone formation between these composites were observed at an orthotopic implantation site. This is in line with the limited studies investigating BMP-2 release in various biomaterials such as calcium phosphate cement (ceramic), gelatin (natural polymer), and OPF (synthetic polymer), suggesting that an initial burst release is favorable for BMP-2-induced bone formation at a



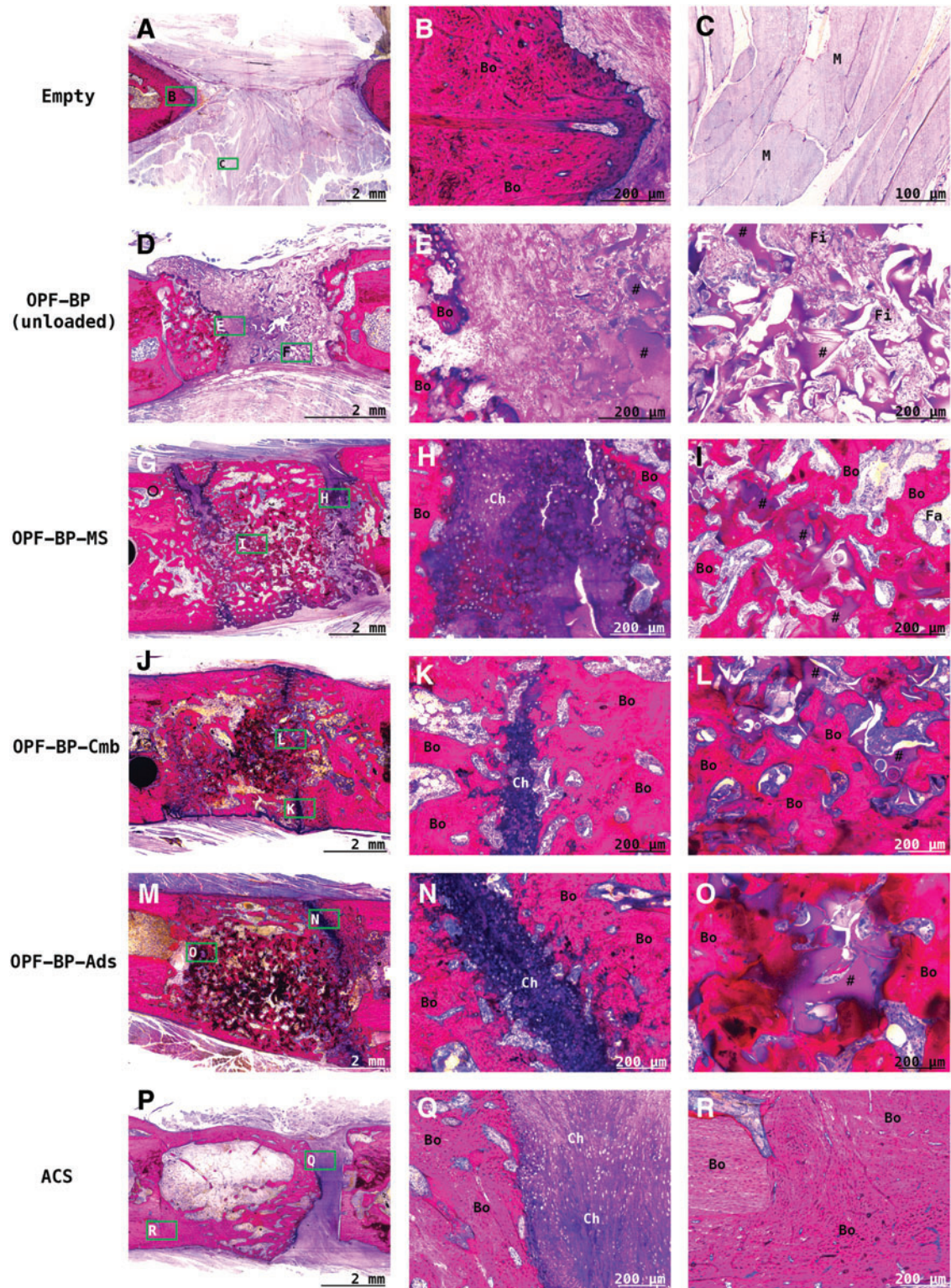


**FIG. 5.** Representative methylene blue/basic fuchsin-stained histological sections of the implants after 9 weeks of orthotopic implantation. In the empty defect (A–C), there was interposition of muscle tissue (M) in the center of the empty femoral defect with limited ingrowth of bone (Bo) from the distal and proximal osteotomy sides. The unloaded OPF-BP composites (#) (D–F) showed ingrowth of fibrous tissue (Fi) in the pores with bone formation at both osteotomy sides. In all BMP-2-loaded OPF-BP composites (G–O) (#), a combination of endochondral (Ch), woven, and lamellar bone formation was seen with fat cells (Fa) centrally in the pores. The ACS (P–R) was fully resorbed and the defect was mainly filled with chondrocytes and woven and lamellar bone. Green squares represent approximate locations of the high-magnification images. Empty: unfilled defect, OPF-BP: unloaded control, OPF-BP-MS: microsphere (more sustained BMP-2 release), OPF-BP-Cmb: combined (combined BMP-2 release), OPF-BP-Ads: adsorbed (mainly burst release), ACS: absorbable collagen sponge containing 2  $\mu$ g BMP-2 (mainly burst release) as positive control. Color images are available online.



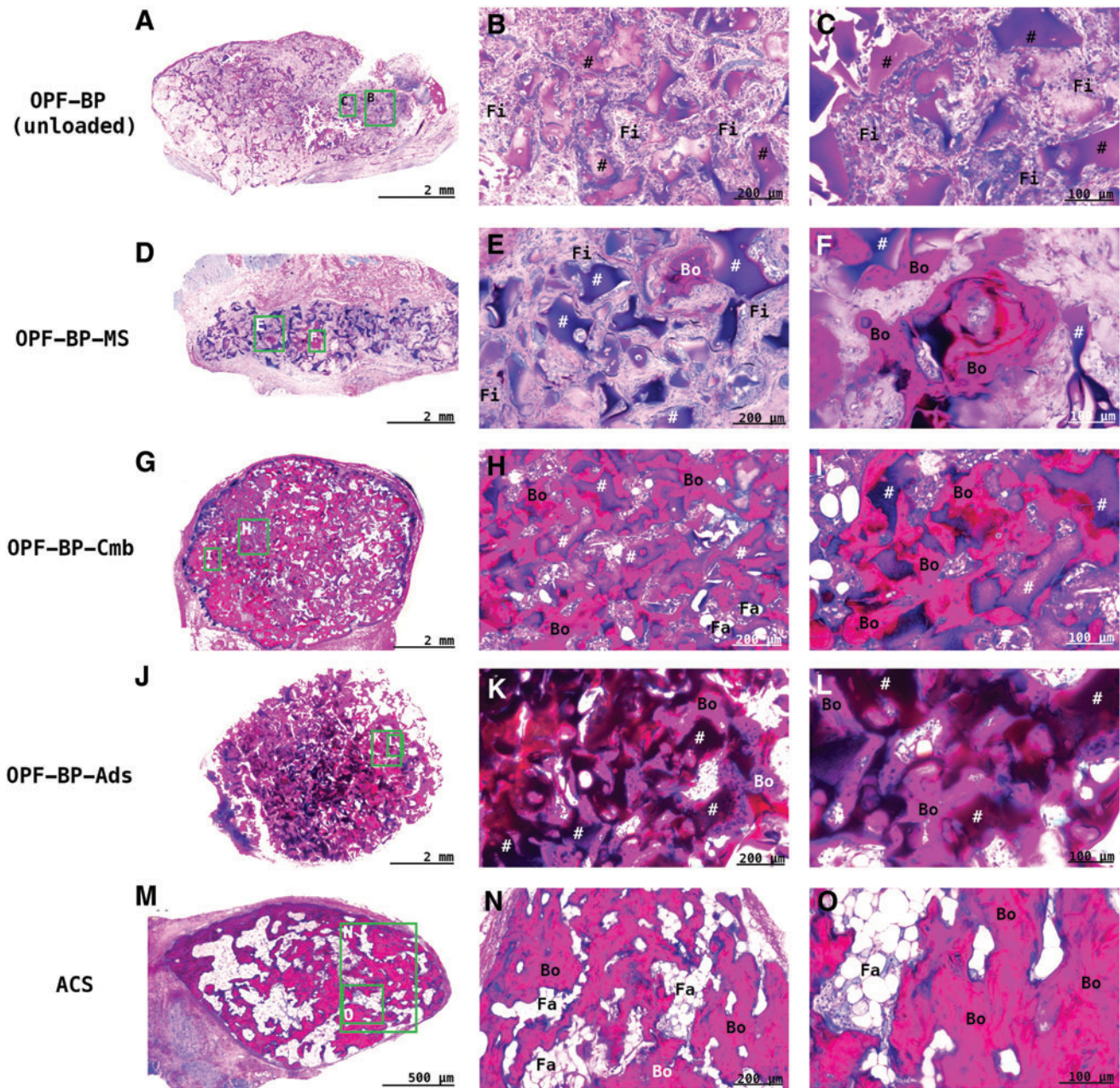


**FIG. 6.** Methylene blue/basic fuchsin-stained histological sections of the implants after 9 weeks of subcutaneous implantation. The pictures shown are representative for the groups. The unloaded OPF-BP (A–C) hydrogels (#) formed an interconnected porous network without any bone formation and mainly ingrowth of fibrous tissue (Fi). In BMP-2 containing OPF-BP composites, ingrowth of fibrous tissue, fat tissue (Fa), and bone (Bo) was seen. Whereas only small bony islands surrounded by fibrous tissue were seen in OPF-BP-MS (D–F), good bone ingrowth was seen in OPF-BP-Cmb (G–I) and OPF-BP-Ads (J–L) with bone and osteoid growing on the surface of the hydrogel with fat cells centrally in the pores. The ACS (M–O) was fully resorbed and replaced by small ossicles with a thin cortex containing trabecular bone structure and fat cells centrally. *Green squares* represent approximate locations of the high-magnification images. OPF-BP: unloaded control, OPF-BP-MS: microsphere (more sustained BMP-2 release), OPF-BP-Cmb: combined (combined BMP-2 release), OPF-BP-Ads: adsorbed (mainly burst release), ACS: absorbable collagen sponge containing 2  $\mu$ g BMP-2 (mainly burst release) as positive control. Color images are available online.

subcutaneous application site.<sup>8,12,18</sup> However, the present study indicates that a more sustained release profile generates comparable bone volume with a BMP-2 burst release in an orthotopic implantation site. Whereas the bone formation rate for all BMP-2-loaded OPF-BP composites was similar until week 6, sustained BMP-2 release from OPF-BP-MS

resulted in a significantly faster bone formation rate for the last 3 weeks.

The question arises as to how the location site affects bone formation. Since a previous study showed limited differences between ectopic and orthotopic measured release profiles,<sup>25</sup> factors at the implantation sites are most

likely responsible for the differences in BMP-2 responsiveness. Mechanisms such as osteoconduction and autologous osteoinduction could enhance the natural bone regeneration process at the orthotopic location compared with the subcutaneous environment. Furthermore, the availability of BMP-2 responsive cells and several locally produced growth factors and cytokines is different for the ectopic and orthotopic locations. The first few days after implantation, the composites are surrounded by a hematoma at both locations.<sup>27</sup> However, the exposed bone marrow at the orthotopic location may generate a hematoma more enriched with pluripotent cells compared with the subcutaneous tissue layer. In line with this thought, multipotent cells in bone marrow are readily available after aspiration, while the multipotent cells after liposuction are still embedded in the fat tissue.<sup>28–30</sup>

Furthermore, whereas both adipose- and bone marrow-derived cells are able to differentiate toward the osteogenic lineage, various *in vitro* studies have suggested an inferior osteogenic capacity of adipose-derived cells.<sup>31,32</sup> Apart from possible local differences in BMP-2 responsive cells, several locally produced growth factors and cytokines may influence the regeneration process at the different sites. In an ectopic environment, the BMP-2 release has to modify the normal regeneration process toward wound healing, while in an orthotopic environment, BMP-2 can act synergistically with a cascade already in favor of bone healing. In line with this, simultaneous release of BMP-2 with vascular endothelial growth factor (VEGF) showed improved bone formation subcutaneous, while similar bone formation was observed in an orthotopic location.<sup>33</sup> Whereas the VEGF could have influenced the subcutaneous environment in favor of bone formation, a sufficient exogenous level of growth factors was available at the orthotopic environment, making the additional release of VEGF not clinically relevant.

While the effect of BMP-2 release kinetics on bone formation was location dependent, the effect of composite chemistry and structure was similar at both application sites. The biomaterial chemistry and structure of OPF-BP enhanced bone formation at both subcutaneous and orthotopic locations. Whereas ACS formed small ossicles subcutaneously and nonbridging defects orthotopically, OPF-BP-Ads with similar BMP-2 release kinetics generated significantly more bone formation in both implantation locations. Also, all OPF-BP composites showed more efficient use of the released BMP-2 after 9 weeks of orthotopic implantation. This emphasizes the role of biomaterials as a scaffold for bone tissue formation, more efficient use of BMP-2, and eventual bridging of bone defects. The phosphate-modified hydrogel functioned as a framework that prohibited interposition of surrounding structures and provided a structure for cells to attach and proliferate. This is in line with *in vitro* results showing that incorporation of phosphate into OPF or PEG improved mineralization, attachment, and proliferation of mesenchymal stem cells and osteoblasts.<sup>19–22</sup>

## Conclusion

In conclusion, this study clearly showed that the osteoinductive effect of different BMP-2 release profiles is location dependent. Whereas BMP-2 sustained release was insufficient to generate adequate bone formation in a subcutaneous environment, good bone formation was seen in an

orthotopic environment. As opposed to BMP-2 release, composite chemistry and structure had a similar influence on bone formation at both subcutaneous and orthotopic application sites. More bone formation in OPF-BP composites compared with ACS at both application sites emphasizes the role of biomaterials as scaffold to achieve proper bone tissue formation.

## Acknowledgments

The authors acknowledge the financial support from the National Institutes of Health (R01 AR45871 and R01 EB03060), the AO Foundation (AO startup grant S-15-46K), the Dutch Arthritis Foundation (LLP12 and LLP22), and Anna-NOREF foundation. Furthermore, the authors thank Nynke Ankringa from the Department of Veterinary Pathology of the University of Utrecht for analyzing histology, and Michiel Croes and Marianne K.E. Koolen from the Department of Orthopedic Surgery of the University Medical Center Utrecht for assisting with the surgery.

## Author Contributions

M.G.L.O., L.L., M.J.Y., W.J.A.D., J.A., and D.H.R.K. designed the study. M.G.L.O., L.L., M.A.T., B.P., L.D.L., B.P.M., and D.H.R.K. participated in data acquisition, analysis, and interpretation. All authors participated in drafting and revising the article.

## Disclosure Statement

No competing financial interests exist.

## References

1. Seeherman, H., Li, R., and Wozney, J. A review of pre-clinical program development for evaluating injectable carriers for osteogenic factors. *J Bone Joint Surg Am* **85(Suppl. 3)**, 96, 2003.
2. Putney, S.D., and Burke, P.A. Improving protein therapeutics with sustained-release formulations. *Nat Biotechnol* **16**, 153, 1998.
3. Hosseinkhani, H., Hosseinkhani, M., Khademhosseini, A., and Kobayashi, H. Bone regeneration through controlled release of bone morphogenetic protein-2 from 3-D tissue engineered nano-scaffold. *J Control Release* **117**, 380, 2007.
4. Rodríguez-Évora, M., Delgado, A., Reyes, R., *et al.* Osteogenic effect of local, long versus short term BMP-2 delivery from a novel SPU-PLGA-betaTCP concentric system in a critical size defect in rats. *Eur J Pharm Sci* **49**, 873, 2013.
5. Yamamoto, M., Takahashi, Y., and Tabata, Y. Controlled release by biodegradable hydrogels enhances the ectopic bone formation of bone morphogenetic protein. *Biomaterials* **24**, 4375, 2003.
6. Yamamoto, M., Tabata, Y., and Ikada, Y. Ectopic bone formation induced by biodegradable hydrogels incorporating bone morphogenetic protein. *J Biomater Sci Polym Ed* **9**, 439, 1998.
7. Gothard, D., Smith, E.L., Kanczler, J.M., *et al.* Tissue engineered bone using select growth factors: a comprehensive review of animal studies and clinical translation studies in man. *Eur Cells Mater* **28**, 166, 2014. discussion 208.
8. Kempen, D.H., Lu, L., Hefferan, T.E., *et al.* Retention of *in vitro* and *in vivo* BMP-2 bioactivities in sustained

- delivery vehicles for bone tissue engineering. *Biomaterials* **29**, 3245, 2008.
9. Hernández, A., Sánchez, E., Soriano, I., Reyes, R., Delgado, A., and Évora, C. Material-related effects of BMP-2 delivery systems on bone regeneration. *Acta Biomater* **8**, 781, 2012.
  10. Piskounova, S., Gedda, L., Hulsart-Billström, G., Hilborn, J., and Bowden, T. Characterization of recombinant human bone morphogenetic protein-2 delivery from injectable hyaluronan-based hydrogels by means of <sup>125</sup>I-radiolabelling. *J Tissue Eng Regen Med* **8**, 821, 2014.
  11. Ruhé, P.Q., Boerman, O.C., Russel, F.G., Mikos, A.G., Spauwen, P.H., and Jansen, J.A. In vivo release of rhBMP-2 loaded porous calcium phosphate cement pretreated with albumin. *J Mater Sci Mater Med* **17**, 919, 2006.
  12. van de Watering, F.C., Molkenboer-Kuening, J.D., Boerman, O.C., van den Beucken, J.J., and Jansen, J.A. Differential loading methods for BMP-2 within injectable calcium phosphate cement. *J Control Release* **164**, 283, 2012.
  13. Woo, B.H., Fink, B.F., Page, R., *et al.* Enhancement of bone growth by sustained delivery of recombinant human bone morphogenetic protein-2 in a polymeric matrix. *Pharm Res* **18**, 1747, 2001.
  14. Yamamoto, M., Ikada, Y., and Tabata, Y. Controlled release of growth factors based on biodegradation of gelatin hydrogel. *J Biomater Sci Polym Ed* **12**, 77, 2001.
  15. Takita, H., Vehof, J.W., Jansen, J.A., *et al.* Carrier dependent cell differentiation of bone morphogenetic protein-2 induced osteogenesis and chondrogenesis during the early implantation stage in rats. *J Biomed Mater Res A* **71**, 181, 2004.
  16. Tazaki, J., Murata, M., Akazawa, T., *et al.* BMP-2 release and dose-response studies in hydroxyapatite and beta-tricalcium phosphate. *Biomed Mater Eng* **19**, 141, 2009.
  17. Ruhé, P.Q., Boerman, O.C., Russel, F.G., Spauwen, P.H., Mikos, A.G., and Jansen, J.A. Controlled release of rhBMP-2 loaded poly(dl-lactic-co-glycolic acid)/calcium phosphate cement composites in vivo. *J Control Release* **106**, 162, 2005.
  18. Olthof, M.G.L., Kempen, D.H.R., Liu, X., *et al.* Bone morphogenetic protein-2 release profile modulates bone formation in phosphorylated hydrogel. *J Tissue Eng Regen Med* **12**, 1339, 2018.
  19. Nuttelman, C.R., Benoit, D.S., Tripodi, M.C., and Anseth, K.S. The effect of ethylene glycol methacrylate phosphate in PEG hydrogels on mineralization and viability of encapsulated hMSCs. *Biomaterials* **27**, 1377, 2006.
  20. Dadsetan, M., Giuliani, M., Wanivenhaus, F., Brett Runge, M., Charlesworth, J.E., and Yaszemski, M.J. Incorporation of phosphate group modulates bone cell attachment and differentiation on oligo(polyethylene glycol) fumarate hydrogel. *Acta Biomater* **8**, 1430, 2012.
  21. Dalby, M.J., Gadegaard, N., Tare, R., *et al.* The control of human mesenchymal cell differentiation using nanoscale symmetry and disorder. *Nat Mater* **6**, 997, 2007.
  22. Müller, P., Bulnheim, U., Diener, A., *et al.* Calcium phosphate surfaces promote osteogenic differentiation of mesenchymal stem cells. *J Cell Mol Med* **12**, 281, 2008.
  23. Olthof, M.G.L., Tryfonidou, M., Liu, X., *et al.* Phosphate functional groups improve OPF osteoconduction and BMP-2 osteoinductive efficacy. *Tissue Eng Part A* **24**, 819, 2018.
  24. Seeherman, H., and Wozney, J.M. Delivery of bone morphogenetic proteins for orthopedic tissue regeneration. *Cytokine Growth Factor Rev* **16**, 329, 2005.
  25. Kempen, D.H., Lu, L., Classic, K.L., *et al.* Non-invasive screening method for simultaneous evaluation of in vivo growth factor release profiles from multiple ectopic bone tissue engineering implants. *J Control Release* **130**, 15, 2008.
  26. Hoaglin, D.C., Iglewicz, B., and Tukey, J.W. Performance of some resistant rules for outlier labeling. *J Am Stat Assoc* **81**, 991, 1986.
  27. McKibbin, B. The biology of fracture healing in long bones. *J Bone Joint Surg Br* **60-B**, 150, 1978.
  28. Aust, L., Devlin, B., Foster, S.J., *et al.* Yield of human adipose-derived adult stem cells from liposuction aspirates. *Cytotherapy* **6**, 7, 2004.
  29. Pittenger, M.F., Mackay, A.M., Beck, S.C., *et al.* Multi-lineage potential of adult human mesenchymal stem cells. *Science* **284**, 143, 1999.
  30. Zhu, Y., Liu, T., Song, K., Fan, X., Ma, X., and Cui, Z. Adipose-derived stem cell: a better stem cell than BMSC. *Cell Biochem Funct* **26**, 664, 2008.
  31. Liao, H.T., and Chen, C.T. Osteogenic potential: comparison between bone marrow and adipose-derived mesenchymal stem cells. *World J Stem Cells* **6**, 288, 2014.
  32. Yang, H.J., Kim, K.J., Kim, M.K., *et al.* The stem cell potential and multipotency of human adipose tissue-derived stem cells vary by cell donor and are different from those of other types of stem cells. *Cells Tissues Organs* **199**, 373, 2014.
  33. Kempen, D.H., Lu, L., Heijink, A., *et al.* Effect of local sequential VEGF and BMP-2 delivery on ectopic and orthotopic bone regeneration. *Biomaterials* **30**, 2816, 2009.

Address correspondence to:  
 Diederik H.R. Kempen, MD, PhD  
 Department of Orthopaedic Surgery  
 Onze Lieve Vrouwe Gasthuis  
 Oosterpark 9  
 Amsterdam, 1091 AC  
 The Netherlands

E-mail: d.h.r.kempen@olv.gn

Received: October 16, 2017

Accepted: June 21, 2018

Online Publication Date: January 25, 2019